Available online at www.sciencedirect.com

ScienceDirect

Advances in Space Research 61 (2018) 777–785

ADVANCES IN SPACE RESEARCH (a COSPAR publication)

www.elsevier.com/locate/asr

Solar flares, CMEs and solar energetic particle events during solar cycle 24

Bimal Pande, Seema Pande *, Ramesh Chandra, Mahesh Chandra Mathpal

Department of Physics, DSB Campus, Kumaun University, Nainital 263 001, India

Received 25 March 2017; received in revised form 16 November 2017; accepted 20 November 2017
Available online 27 November 2017

Abstract

We present here a study of Solar Energetic Particle Events (SEPs) associated with solar flares during 2010–2014 in solar cycle 24. We have selected the flare events (≥GOES M-class), which produced SEPs. The SEPs are classified into three categories i.e. weak (proton intensity ≤ 1 pfu), minor (1 pfu < proton intensity < 10 pfu) and major (proton intensity ≥ 10 pfu). We used the GOES data for the SEP events which have intensity greater than one pfu and SOHO/ERNE data for the SEP event less than one pfu intensity. In addition to the flare and SEP properties, we have also discussed different properties of associated CMEs.

Keywords: Solar energetic particles; Coronal mass ejections; Flares

1. Introduction

Solar energetic particles (SEPs) are one of the important phenomena associated with the solar eruptions for example: solar flares, filament eruptions, coronal mass ejections (CMEs), etc. Their energy ranges from keV to GeV. CME speed, magnetic connectivity to Earth, and ambient magnetic conditions are responsible for the intensities of SEPs (Gopalswamy et al., 2014).

According to previous studies, it is found that the SEPs can be generated by the shock ahead of the CMEs (Reames, 1999). Strong SEPs show close association with halo CMEs and the average speed of the associated CMEs are ~1500 km/s (Gopalswamy et al., 2014). Faster CMEs drive stronger shocks; therefore, there should be good correlation between the CME speed and the SEP intensity. However, this relation is not very good. The reason for these discrepancies is not well understood. Gopalswamy et al. (2012) have discussed various factors behind this poor correlation for example: CME-CME interaction, deflection of CMEs from the coronal hole regions, etc.

Another important mechanism for the generation of SEPs is the magnetic reconnection manifested as solar flares (Cane et al., 1986). It is believed that the particle acceleration in flare occurs in the low corona. The magnetic field is closed in active regions. This implies that energetic particles do not have direct access to open Interplanetary magnetic field (IMF). Therefore, the magnetic reconnection that accelerates the SEPs should include closed and open magnetic flux systems (Reames, 2002, Masson et al., 2013). Studies have been done for the comparison of soft X-ray emission and its SEP associations (Gopalswamy et al., 2003; Miteva et al., 2013; Trottet et al., 2015). These studies show that there is a weak correlation between GOES X-ray flare size and the SEP intensities. Miteva et al. (2013) have conducted a statistical study between the peak intensities of particle events and the parameters of the associated coronal activity such as soft X-ray (SXR) flux of the flare, CME speed and width. They found

* Corresponding author.
E-mail address: pande.seema@yahoo.com (S. Pande).

https://doi.org/10.1016/j.asr.2017.11.025
0273-1177/

that the correlation is better when the SEPs are detected within an Interplanetary Coronal Mass Ejection (ICME) rather than when they propagate in the ambient solar wind.

It is also interesting to compare microwave emission produced by non-thermal electrons with SEPs. The reason for this is that the microwave emission during solar flares can tell more about the particle acceleration. Another evidence which confirms that SEPs are associated with reconnection is there association with type III radio bursts observed by various ground as well as space borne instruments. The association of type III radio bursts with SEPs suggests that charged particles can escape to the interplanetary space (Wild et al. (1963), Buttighoffer (1998), Miteva et al. (2014) and Winter and Ledbetter (2015), references cited therein). Flare associated SEPs are impulsive in nature, however, shock associated SEPs are gradual in nature. Gopalswamy et al. (2014) found that only 27% of the GOES major flares (≥M GOES class) were associated with SEPs. Dierckxsens et al. (2015) did a statistical analysis of SEPs and their properties with solar flare and CMEs during the solar cycle 23 for low (>10 MeV) and high (>60 MeV) energy range. They found the CMEs speed/flare intensity is strongly/weakly correlated with SEPs intensity for the low energy range. Using the SOHO/ERNE 55–80 MeV data Paassilta et al. (2017) performed the study of SEPs during solar cycle 23 and 24 and compared the properties of SEPs with flare and CMEs characteristics. The different characteristics of SEPs and their relation with other solar activities are extensively described in the review paper by Reames (2013). Therefore, from the above discussion it is inferred that none of the mechanism i.e. neither shock nor magnetic reconnection is solely responsible for the generation of SEPs.

In this paper we have selected the SEP events of the period 2010–2014, which are associated with solar flares having magnitude greater than GOES M-class (peak flux range 10^{-5}–10^{-4} W/m^2). In this article, we plan to study the role of the magnetic reconnection and shock mechanism for the generation of SEPs. The main difference between our study and earlier studies on SEPs events of the current cycle is that the previous studies used the SEPs data for the major (proton intensity ≥ 10 pfu) while in our present study, we have selected minor and weak (proton i ntensity < 1 pfu) events also. The paper is organized as follows: Section 2 presents the observations and data selection criteria, Section 3 describe the results and discussions. The results are summarized in Section 4.

2. Observational data sets

For our study, we have selected solar flares (GOES class ≥ M class) associated with SEP events. We have divided the observed SEP events into three categories, viz., weak (proton intensity ≤ 1 pfu, 1 pfu = 1 proton cm^{-1} s^{-1} sr^{-1}), minor (1 pfu < proton intensity < 10 pfu) and major (proton intensity ≥ 10 pfu).

We have used SEP events data from GOES in the ≥10 MeV energy channel. The SEPs events <1 pfu are not distinguishable in GOES data. Therefore, for these SEP events, we have used the data from the Energetic and Relativistic Nuclei and Electron (ERNE, Torsti et al., 1995) instruments onboard SOHO in 12.6–140 MeV energy range. Due to the high sensitivity of ERNE instrument, it is useful for the weaker SEPs. Following Chandra et al. (2013), we have converted the ERNE data into pfu. **The identification of the SEPs is based on the onset time of proton flux > 10 MeV. We have selected the SEP events when the proton flux becomes substantially larger than the average background flux value.**

We have downloaded the GOES data from http://sec.noaa.gov, while the SOHO/ERNE data are available at http://www.srl.utu.fi/erne_data/datafinder/df.shtml. The CME data are downloaded from the Large Angle and Spectrometric Coronagraph (LASCO, Brueckner et al., 1995) onboard SOHO (http://cdaw.gsfc.nasa.gov, Gopalswamy et al., 2009). The CME solar source location was searched using available images, movies and Solar Geophysical data (SGD) list: for example the images and movies from the Solar Dynamic Observatory (SDO).

For the X-ray and optical classification, we have used the event lists from the SGD. The metric type II burst data obtained by various ground based instruments are available online (ftp://ftp.ngdc.noaa.gov/STP/SOLAR_DATA/SOLAR_RADIO/SPECTRAL/).

The total selected events using above discussed criteria are 35 and listed in Table 1. Figs. 1–3 presents the examples of a major, minor, and weak SEP event and its solar source region.

3. Results and discussion

In this section, we describe the properties of flares, associated SEPs and CMEs. The solar source regions is also discussed. The detailed description is presented in following subsections.

3.1. Flare characteristics

Here, we compare the GOES X-ray flare intensities with the SEP events. For the flare size, we use the peak soft X-ray flux (in units of W m^{-2}) in the GOES 1–8 Å channel. We found 26 (74 %) were associated with GOES M-class; whereas 09 (26%) were associated with GOES X-class solar flares. During our study period we found 54%, 29% and 17% SEPs were major, minor and weak respectively. This indicates that the flare size may not be the only good indicator of SEPs.

In Fig. 4 (left), we have plotted the GOES X-ray peak flux against the proton intensity. The correlation coefficient between the X-ray peak flux and proton intensity is 0.39, which shows that they are very poorly correlated as reported in earlier observations (Gopalswamy et al.,

Table 1
SEPs associated with ≥ GOES M class flares during 2010–2014.

S.N.	Date	SEP Time (UT)	CME			Location	Proton flux (pfu)	AR	Flare Class	Flare onset
			Time (UT)	Speed (km/s)	Width (degree)					
1	100612	03:30	01:31	486	119	N23W43	0.5 (w)	11081	M2.0	00:30
2	100807	20:22	18:36	871	H	N11E34	0.5 (w)	11093	M1.0	17:55
3	110128	01:00	01:25	606	119	N13W93	2.8 (m)	11149	M1.3	00:44
4	110215	03:00	02:24	669	H	S20W12	2.5 (m)	11158	X2.2	01:44
5	110307	21:50	20:00	2125	H	N30W47	12 (M)	11164	M3.7	19:43
6	110607	08:20	06:49	1255	H	S21W54	73 (M)	11226	M2.5	06:16
7	110802	07:00	06:36	712	268	N14W15	4 (m)	11261	M1.4	05:19
8	110803	14:42	14:00	610	H	N17W30	1 (m)	11261	M6.0	13:17
9	110804	05:16	04:12	1315	H	N19W36	60 (M)	11261	M9.3	03:41
10	110808	19:05	18:12	1343	237	N16W61	4 (m)	11263	M3.5	18:00
11	110809	08:45	08:12	1610	H	N17W69	26 (M)	11263	X6.9	07:48
12	110906	02:30	02:24	782	H	N14W07	1 (m)	11283	M5.3	01:35
13	110906	00:00[a]	23:05	575	H	N14W18	9 (m)	11283	X2.1	22:12
14	111225	20:00	18:48	366	125	S22W26	5 (m)	11387	M4.0	18:11
15	120127	18:55	18:27	2508	H	N27W71	795 (M)	11402	X1.7	17:37
16	120307	0250	00:24	2684	H	N17E27	1500 (M)	11429	X5.4	00:02
17	120313	1805	1736	1884	H	N17W66	469 (M)	11429	M7.9	17:12
18	120517	0155	0148	1582	H	N11W76	255 (M)	11476	M5.1	01:25
19	120706	0005[a]	2324	1828	H	S13W59	25 (M)	11515	X1.1	23:01
20	120708	1810	1654	1495	157	S17W74	19 (M)	11515	M6.9	16:43
21	120719	0640	0424	444	11	S13W88	80 (M)	11520	M7.7	04:17
22	130305	0845	1012	569	59	S15W54	0.27 (w)	11686	M1.2	07:47
23	130315	1940	0712	1063	H	N11E12	16 (M)	11692	M1.1	05:46
24	130411	0825	0724	861	H	N09E12	114 (M)	11719	M6.5	06:55
25	130623	0830	2124	339	101	S15E62	14 (M)	11778	M2.9	20:48
26	130817	2015	1912	1202	H	S05W30	0.20 (w)	11818	M1.4	18:49
27	131022	2121	2148	459	H	N04W01	0.75 (w)	11875	M4.2	21:15
28	131025	0854	0812	438	H	S06E69	7.42 (m)	11882	X1.7	07:53
29	140107	1955	1824	1830	H	S15W11	1026 (M)	11944	X1.2	18:04
30	140220	0815	0804	948	H	S15W73	22 (M)	11976	M3.0	07:26
31	140225	0350	0125	2147	H	S12E62	24 (M)	11990	M4.9	00:39
32	140418	1340	1331	1203	H	S20W34	58 (M)	12036	M7.3	12:31
33	140507	1732	1624	923	H	N15E50	0.8 (w)	12051	M1.2	16:07
34	140612	2336	2200	970	58	S20W55	3.69 (m)	12085	M3.1	21:34
35	140910	2135	1800	1425	H	N14E02	20 (M)	12158	X1.6	17:21

[a] Indicates the next day time.

2003, 2004; Chandra et al., 2013). In the same figure (right) we have shown the same plot for the events, which are associated with the halo CMEs. We note that the correlation coefficient become 0.16, which is weaker now. This poor correlation could be due to the weak acceleration of the particles during the solar flares. This can be checked by looking into the intensity of microwave emission and their association with type III radio bursts. However, this is out of the scope of this paper. Another possibility for the poor correlation was given by Gopalswamy et al. (2003). In their study they have proposed that due to the halo CMEs it is possible that the shock becomes strong and hence the contribution from the shock is stronger. Many cases have been reported in the literature, when there is no flare and only fast CMEs are observed, which could be associated with filament eruptions (Kahler et al., 1978; Giacalone, 2012; Reames, 2012; Gopalswamy et al., 2015). Therefore, when there is high speed halo CME, the contribution towards the SEPs production is more in comparison to solar flares.

3.2. SEPs intensities

Fig. 5 presents the longitude of the source regions (left) and intensities (right) of the SEPs with the number of SEPs. We have noticed the majority of the SEP source regions are located in the western hemisphere, which confirm the previous results (Gopalswamy et al., 2008; Manoharan and Agalya, 2011, Chandra et al., 2013). The mean values of SEP intensity is 283.23 pfu. There are five events having eastern hemispheric source regions (≥30° longitude). The occurrence of above eastern hemisphere source regions associated with SEPs can be explained either due to the deflection from the radial direction of the eruptions from coronal holes or due to the interaction of CMEs which are close in time and source locations. There are observations, where the eruptions can reflect up to 90° (Zuccarello et al., 2017).

In our data sets, there are two events one on 07 March 2012 SEP intensity 1500 pfu and another on 07 January 2014 SEP intensity 1026 pfu. The speeds of associated

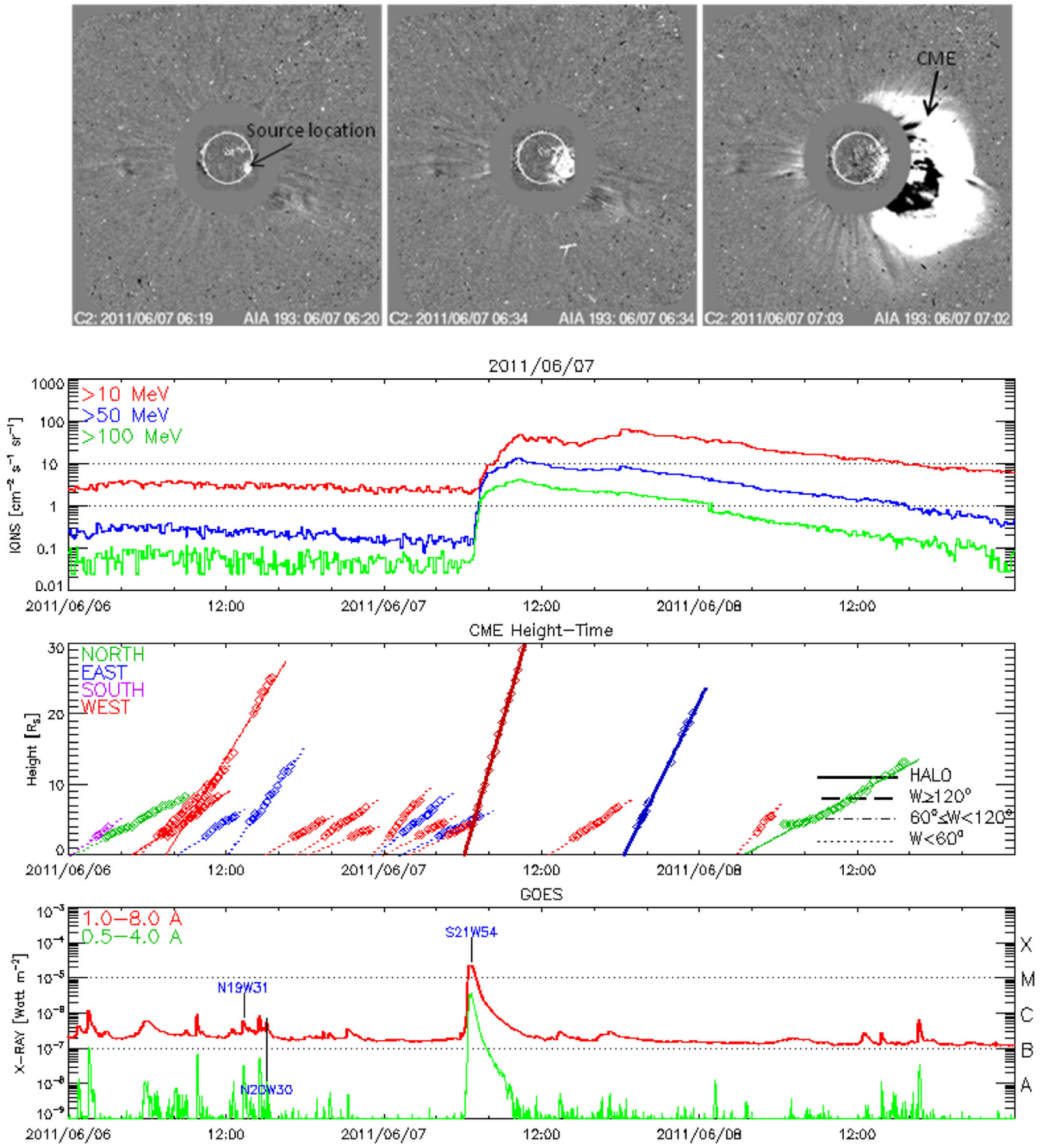

Fig. 1. An example of major SEP event and its source region on 07 June 2011: Images of the CME evolution that produced the SEP event (first panel), the time variation of SEP intensity in three energy channels (second panel), the CME height-time plot (third panel), and the soft X-ray flare light curves in the two energy channels (fourth panel).

CMEs were 2684 and 1830 km/s respectively. Together with the CME speed the SEPs event of 07 March 2012 was associated with stronger flare class i.e. GOES X5.4 and the event of 07 January 2014 was associated with relatively weaker GOES X1.2 class flare. That could be another possibility for the more intense SEP on 07 March 2012. However, we could not expand our logic for all the major SEPs. Moreover, all major SEPs are associated with stronger CMEs speed which supports the idea proposed by Gopalswamy et al. (2014). **The observed speed of the**

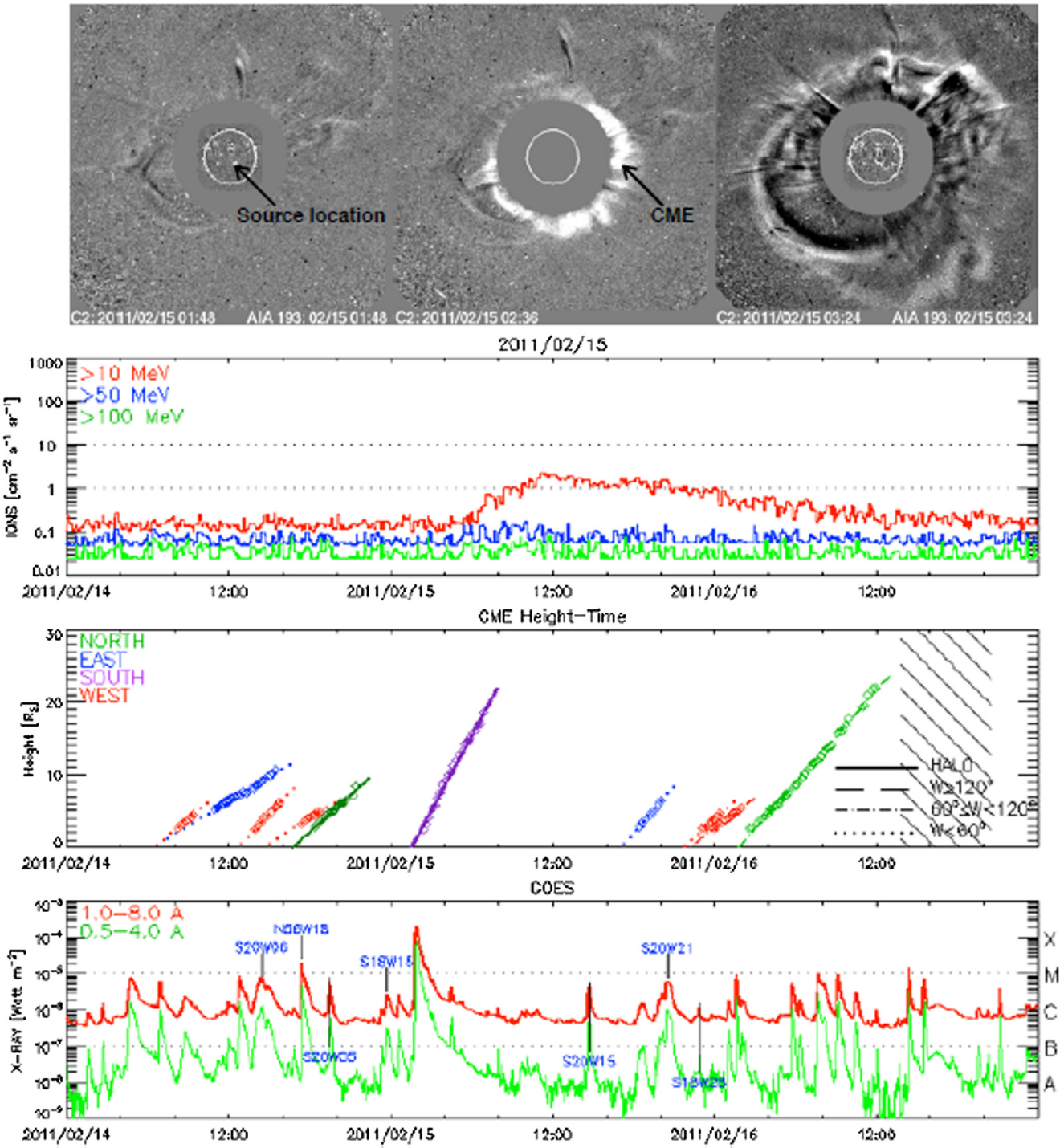

Fig. 2. Same as in Fig. 1 for a minor SEP event and its source region on 15 February 2011.

CME is derived based on the height-time computation observed by the SOHO/LASCO C2 and C3 data. The mentioned speed is average CME speed.

We have also computed the time lag between the onset time of flare and the SEPs. The bar plot between these two are plotted in the Fig. 6. The average time-lag is about three hours. The minimum and maximum time-lag was one and five hours respectively. The reason behind this time-lag could be the flare onset time being at the solar surface while the SEPs onset time is based on the observations of proton flux, when it reaches at the SOHO or GOES satellites.

3.3. CME properties

In Fig. 7, we have plotted the speed of CMEs associated with SEPs against the proton intensity. The left plot is for the total events and the right plot is for the events associated with halo CMEs. We have found that the correlation

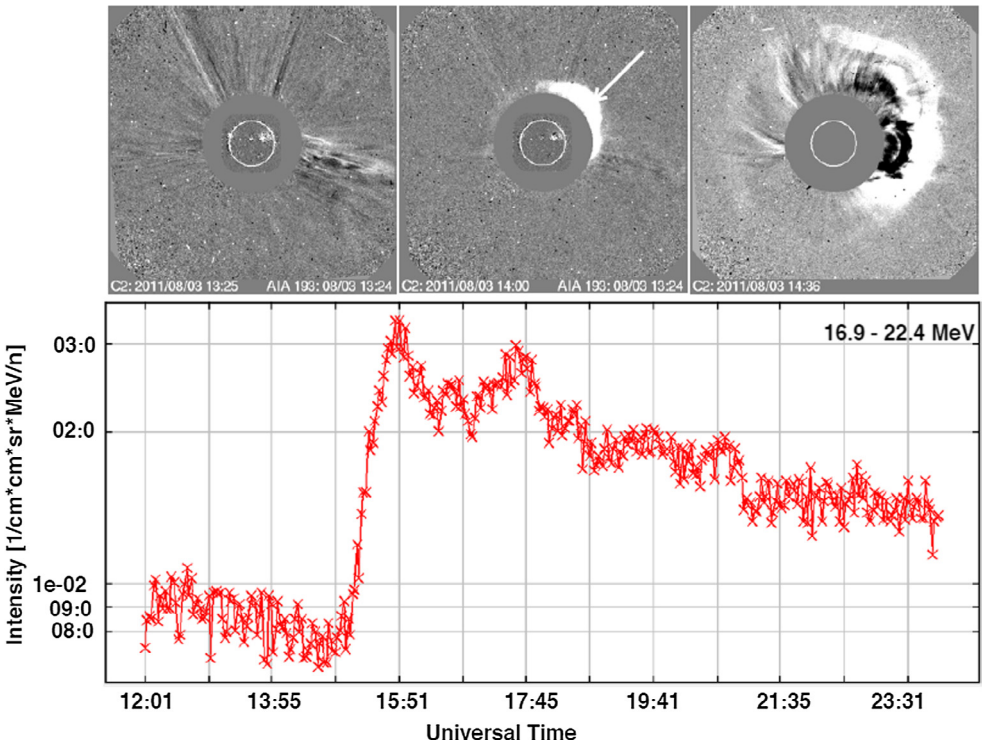

Fig. 3. An example of weak SEP event on 03 August 2011 observed by SOHO/SERNE instrument and its source region: Images of the CME evolution that produced the SEP event (first panel), the time variation of SEP intensity in energy (16.9–22.4 MeV) channel (second panel).

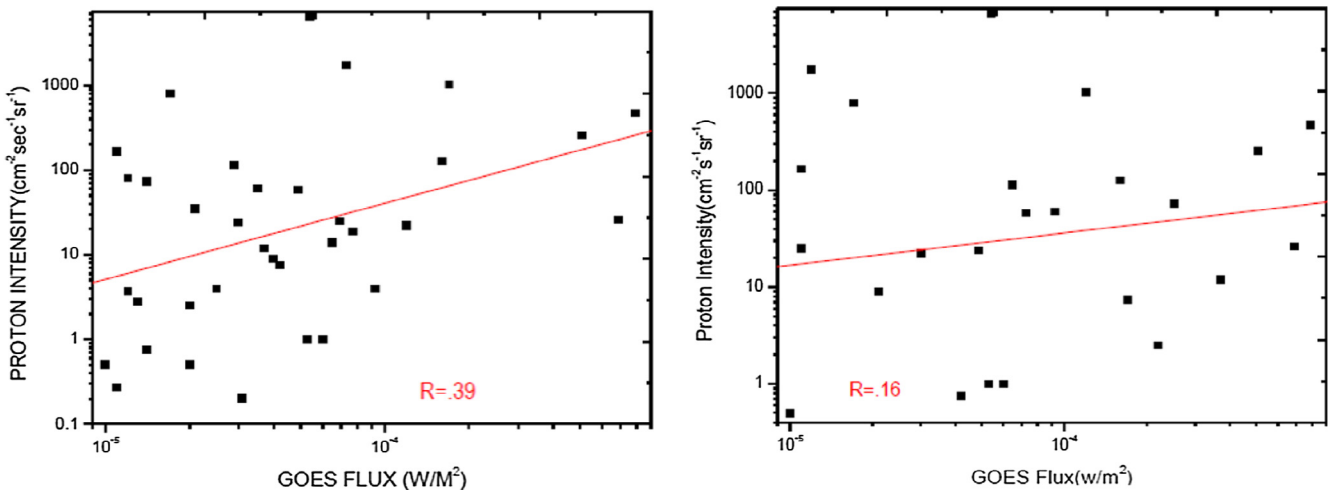

Fig. 4. Left: Scatter plots between X-ray peak flux and proton intensity. Right: Scatter plots between X-ray peak flux and proton intensity for the events associated with halo CMEs. The regression line, correlation coefficients are also shown in the figure.

coefficient between CME speed and peak proton flux during SEPs is 0.53. This weak correlation coefficient can be explained as follows: We have selected the events, which are associated with the M and X-class solar flares. The weak correlation may be due to strong contribution from the reconnection i.e. solar flares. In four of the events there is no type II radio bursts i.e. no indication of shock. Fig. 7 (right) presents the scattered plot between halo CME speed and the proton intensity. The correlation coefficient is now **slightly** improved and the value is 0.60 which can be attributed to the strong shock originating from halo CME. However, there are cases where the strong SEPs were observed only with filament eruption which was associated with weak flare events (for example see. Gopalswamy et al., 2015). In this case the shock was very strong.

Fig. 8 (left) presents distribution of CME speed and SEP intensity. The average speed of CMEs is 1360 km/s. **The width of CMEs coincident with SEP is shown in** Fig. 8 **(right).** The mean widths of the CMEs are 185°. There is no trend as such that the wider CMEs produce more SEPs.

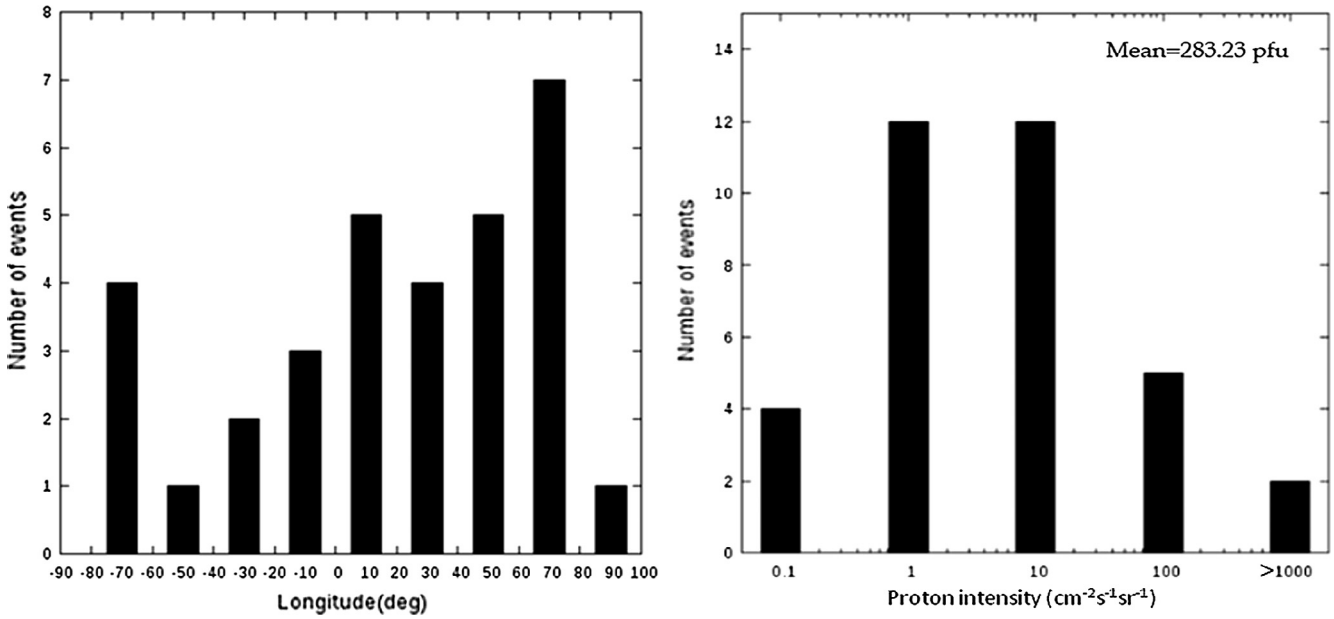

Fig. 5. SEPs source region longitude (left panel), and SEPs intensity (right).

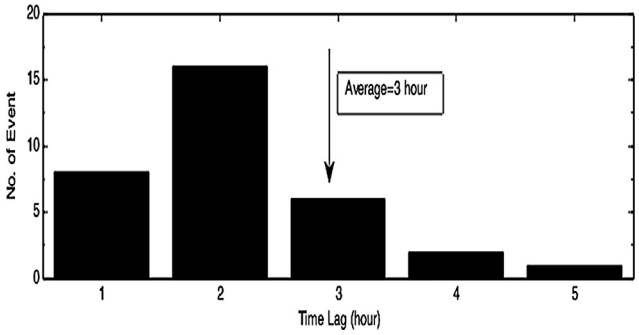

Fig. 6. Time-lag between the flare onset and the SEPs onset.

Nevertheless, majority of SEPs were associated with halo CMEs. The percentage of the halo CMEs decrease when we move from major to weak SEPs. Some of the associated CME properties are summarized in Table 2.

The various computed properties of CMEs for the major, minor, and weak SEPs are given in Table 2. The average CME speed associated with major SEPs is 1500 km/s, which is consistent with the speed derived by Gopalswamy et al. (2014), however they have studied the SEP events of strong intensity only. For minor and weak SEPs the average CME speeds are comparable.

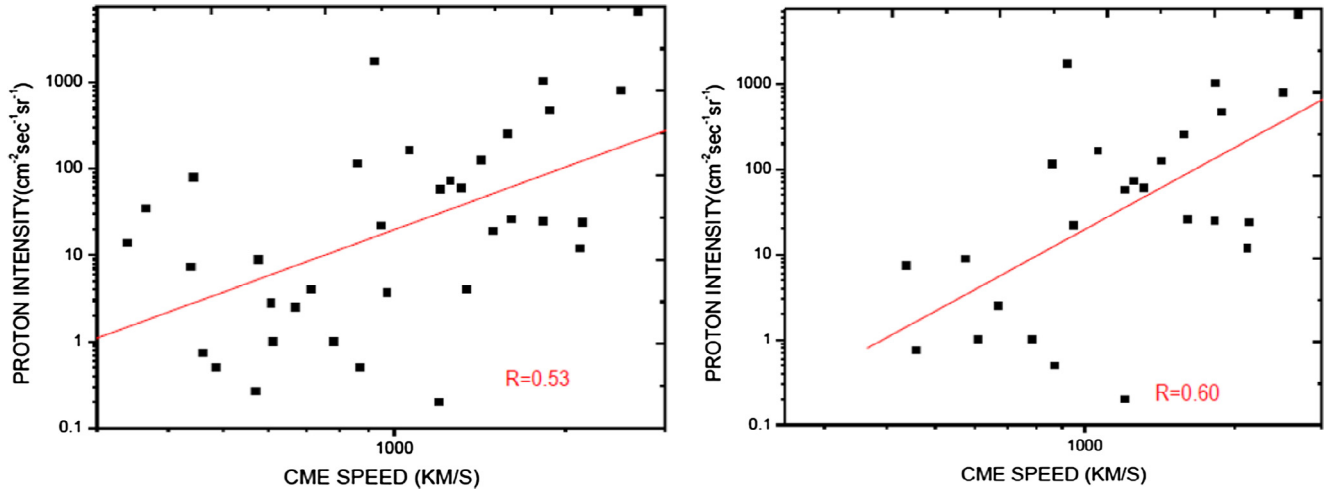

Fig. 7. Left: Scatter plots CME speed and proton intensity. Right: Scatter plots between the halo CMEs speed and proton intensity for the events. The regression line, correlation coefficients are also given in the figure.

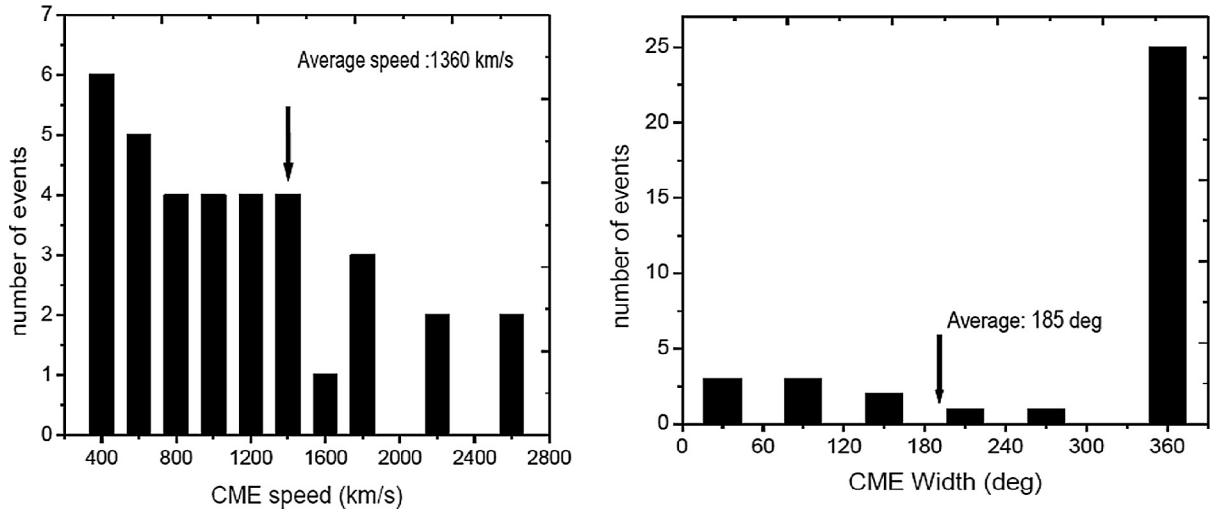

Fig. 8. Properties of CMEs associated with SEPs: Speed (left) and widths (right).

Table 2
Summary of results.

Property	Major	Minor	Weak
No. of SEPs	19	08	08
Average CME speed (km/s)	1500	690	717
No. of halos	16	05	04
Width >120°	01	03	Nil
Width <120°	02	02	02

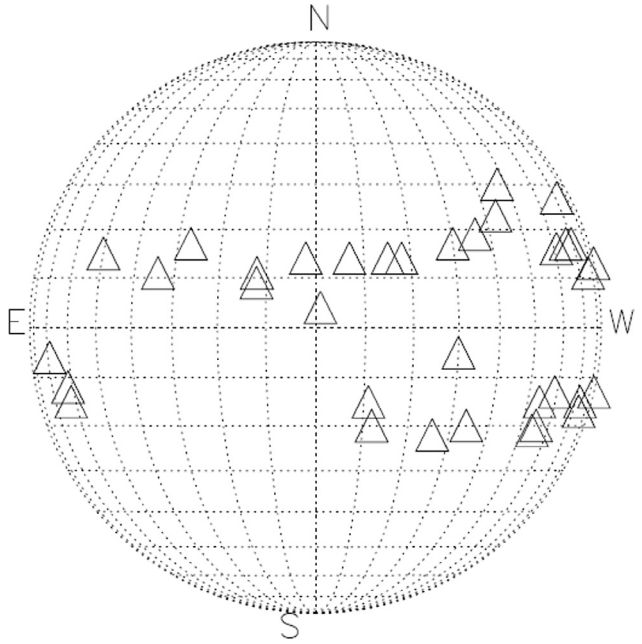

Fig. 9. Locations of SEPs sources on the solar disk.

For the major SEP around 16 out of 19 events are associated with halo CMEs. For minor SEPs around five out of eight events are halos. In case of weak SEP events four out of eight SEPs are associated with halo CME. The narrow widths (<120°) CMEs are associated with two major SEPs. For the narrow CMEs two events are associated with minor and two events are associated with weak SEPs respectively.

The North-South asymmetry of the solar activity features like: filaments, solar flares, sunspots number etc. are discussed by several authors for different solar cycles (Ebert et al., 2013, Li et al., 2009; Joshi and Joshi, 2004; Verma, 1993; Garcia, 1990). To check the North-South asymmetry, we have examined the location of the SEP source region using the data given in column 5 of Table 1. The location of the SEP source region on the solar disk is displayed in Fig. 9. We have found 20 SEP source regions in the northern hemisphere and 15 SEP source regions in the southern hemisphere which confirms the North-South asymmetry in the SEP locations during our study period. We noticed that majority of source region are located in the northern hemisphere.

4. Summary

In the present paper, we have studied the solar flares (GOES class $\geq$ M class), which are associated with SEPs. We discussed about the flare size, SEP intensities, CMEs speed and their solar source regions during 2010–2014. We summarize our results as follow:

- Majority of SEP events source regions are located in the western hemisphere. Some are in eastern part and their speed is high relative to western event.
- Majority of major SEP events are associated with halo and high speed CMEs. The minor and weak SEPs are associated with relatively poor CMEs speeds.
- Most of the SEPs source regions are in northern hemisphere, which indicates north-south asymmetry in SEPs source locations.
- The correlation is slow between X-ray flux and SEP intensity. The correlation looks better between CME speed and SEP intensity, which supports the earlier results.

- Our study extends the earlier study of Chandra et al. (2013) and Gopalswamy (2012) for the solar cycle 24. The poor correlation between X-ray flux and SEP intensity, the source region location in the western hemisphere are consistent with the earlier investigations (for example: Gopalswamy et al. (2003); Gopalswamy et al. (2004); Miteva et al. (2013)). Using the source region of SEP, this study confirm the north-south asymmetry, which is frequently reported in the other solar activity features.

Acknowledgement

We wish to thank both the reviewers for their constructive comments and suggestions, which improved the manuscript considerably. We acknowledge the data from GOES, SOHO/ERNE, LASCO and SDO Instruments. RC also acknowledges the support from SERB/DST Project No. SERB/F/7455/2016-17.

References

Brueckner, G.E., Howard, R.A., Koomen, D.J., et al., 1995. The large angle spectroscopic coronagraph (LASCO). Sol. Phys. 162, 357–402.
Buttighoffer, A., 1998. Solar electron beams associated with radio type {III}. A & A 335, 295–302.
Cane, H.V., McGuire, R.E., von Rosenvinge, T.T., 1986. Two classes of solar energetic particle events associated with impulsive and long-duration soft X-ray flares. Astrophys. J. 301, 448–459.
Chandra, R., Gopalswamy, N., Makela, P., et al., 2013. Solar energetic particle events during the rise phases of solar cycles 23 and 24. Adv. Sp. Res. 52, 2102–2111.
Dierckxsens, M., Tziotziou, K., Dalla, S., Patsou, I., Marsh, M.S., Crosby, N.B., Malandraki, O., Tsiropoula, G., 2015. Relationship between Solar energetic particles and properties of flares and CMEs: statistical analysis of solar cycle 23 events. Sol. Phys. 290, 841–874.
Ebert, R.W., Dayeh, M.A., Desai, M.I., McComas, D.J., Pogorelov, N. V., 2013. Hemispheric asymmetries in the polar solar wind observed by Ulysses near the minima of solar cycles 22 and 23. Astrophys. J. 768, 160–169.
Garcia, H.A., 1990. Evidence of solar-cycle evolution of north–south flare asymmetry during cycles 20 and 21. Sol. Phys. 127, 185–197.
Giacalone, J., 2012. Energetic charged particles associated with strong interplanetary shocks. Astrophys. J. 761, 28–37.
Gopalswamy, N., 2012. Factors affecting the intensity of solar energetic particle events. In: Heerikhuisen, J., Li, G., Zank, G. (Eds.), Proc. Tenth annual Astrophysics Conf., vol. 1436. American Institute of Physics, pp. 247–252.
Gopalswamy, N., Yashiro, S., Krucker, S., Stenborg, G., Howard, R.A., 2004. Intensity variation of large solar energetic particle events associated with coronal mass ejections. J. Geophys. Res. 109, A12015.
Gopalswamy, N., Yashiro, S., Lara, A., Kaiser, M.L., Thompson, B.J., Gallagher, P.T., Howard, R.A., 2003. Large solar energetic particle events of cycle 23: a global view. J. Geophys. Res 30 (12), 8015.
Gopalswamy, N., Yashiro, S., Xie, H., et al., 2008. Radio-quiet fast and wide coronal mass ejections. Astrophys. J. 674, 560–569.
Gopalswamy, N., Mäkelä, P., Akiyama, S., et al., 2015. Large solar energetic particle events associated with filament eruptions outside of active regions. Astrophys. J. 806, 8–22.
Gopalswamy, N., Xie, H., Akiyama, S., et al., 2014. Major solar eruptions and high-energy particle events during solar cycle 24. Earth Planets Space 66, 104–118.
Gopalswamy, N., Yashiro, S., Michalek, G., et al., 2009. The SOHO/LASCO CME catalog. Earth Moon Planet. 104, 295–313.
Joshi, B., Joshi, A., 2004. The north–south asymmetry of soft x-ray flare index during solar cycles 21, 22 and 23. Sol. Phys. 261, 343–356.
Kahler, S.W., Hildner, E., Van Hollebeke, M.A.I., 1978. Prompt solar proton events and coronal mass ejections. Sol. Phys. 57, 429–443.
Li, K.J., Gao, P.X., Zhan, L.S., 2009. The long-term behaviour of the north–south asymmetry of sunspot activity. Sol. Phys. 254, 145–154.
Manoharan, P.K., Agalya, G., 2011. High energy solar particle events and their associated coronal mass ejections. In: Duldig, M. (Ed.), Advances in Geosciences, Solar Terrestrial (ST), 27. World Scientific, Singapore, pp. 165–179.
Masson, S., Antiochos, S.K., DeVore, C.R., 2013. A model for the escape of solar-flare-accelerated particles. Astrophys. J. 771, 82–96.
Miteva, R., Klein, K.-L., Malandraki, O., Dorrian, G., 2013. Solar energetic particle events in the 23rd solar cycle: interplanetary magnetic field configuration and statistical relationship with flares and CMEs. Sol. Phys. 282, 579–613.
Miteva, R., Klein, K.-L., Kienreich, I., Temmer, M., Veronig, A., Malandraki, O.E., 2014. Solar energetic particles and associated EIT disturbances in solar cycle 23. Sol. Phys. 10 (1007), 2601–2631.
Paassilta, R., Osku, V., Rami, V., et al., 2017. Catalogue of 55–80 MeV solar proton events extending through solar clycles 23 and 24. J. Space Weather Space Clim. 7, A14–A32.
Reames, D.V., 1999. Particle acceleration at the Sun and in the heliosphere. Space Sci. Rev. 90, 413–491.
Reames, D.V., 2002. Magnetic topology of impulsive and gradual solar energetic particle events. Astrophys. J. 571, L63–L66.
Reames, D.V., 2012. Particle energy spectra at traveling interplanetary shock waves. Astrophys. J. 757, 93–100.
Reames, Donald V., 2013. The two sources of solar energetic particles. Space Sci. Rev. 175, 53–92.
Torsti, J., Valtonen, E., Lumme, M., et al., 1995. Energetic particle experiment ERNE. Sol. Phys. 162, 505–531.
Trottet, G., Samwel, S., Klein, K.-L., et al., 2015. Statistical evidence for contributions of flares and coronal mass ejections to major solar energetic particle events. Sol. Phys. 290, 819–839.
Verma, V.K., 1993. On the north-south asymmetry of solar active cycles. Astrophys. J. 403, 797–800.
Wild, J.P., Smerd, S.F., Weiss, A.A., 1963. Ann. Rev. Astron. Astrophys. 1, 291–366.
Winter, L.M., Ledbetter, K., 2015. Type II and Type III radio bursts and their correlation with solar energetic proton events. Astrophys. J. 809, 105–123.
Zuccarello, F.P., Chandra, R., Schmieder, B., et al., 2017. The transition from eruptive to confined flares in the same active region. A&A 601, A26–A36.